ISSN 2686-7575 (Online)

https://doi.org/10.32362/2410-6593-2020-15-2-67-76

UDC 546.77+ 661.877.22

Molybdenum(VI) oxide: New methods of synthesis and properties

Elena E. Nikishina[@], Elena N. Lebedeva, Dmitry V. Drobot

MIREA – Russian Technological University (M.V. Lomonosov Institute of Fine Chemical Technologies), Moscow, 119571 Russia
[@]Corresponding author, e-mail: helena_nick@mail.ru

Objectives. *The present study aims to develop new methods for the synthesis of molybdenum(VI) oxide, which is a precursor for the synthesis of functional materials, as well as to investigate the physicochemical properties of the resulting oxide phases.*
Methods. *The synthesized phases and the products of their thermolysis were studied by differential thermal analysis, IR spectroscopy, X-ray diffraction analysis, and granulometry.*
Results. *Three methods for the synthesis of molybdenum(VI) oxide were developed, and the physicochemical properties of the oxide phases obtained were studied. The first method consisted in the reaction of molybdenum pentachloride with a 6.0–9.5 mol/L ammonia solution, the second one was the reaction of niobium pentachloride with a sulfuric acid solution, and the third method involved the reaction of ammonium molybdate with nitric acid, affording brown molybdenum(V)* $MoO(OH)_3$ *hydroxide, a bright blue precipitate of molybdenum blue* $MoO_{2.75}$*, and white hydrated oxide* $MoO_3{\cdot}H_2O$*, respectively.*
Conclusions. *A series of thermal and X-ray diffraction analysis demonstrated that in all cases the samples were amorphous phases. Heat treatment at 580 °C of the synthesized phases led to the formation of a rhombic modification of molybdenum trioxide. The lattice parameters and X-ray density were calculated for all thermolysis products. The effect of heat treatment on the particle size of the synthesized samples and their thermolysis products was studied. Particle size analysis demonstrated that particles of different diameters were formed depending on the synthetic method. The smallest particle size (0.3–0.6 µm) was found in molybdenum trioxide, a product of the thermolysis of the sample obtained by the reaction of molybdenum pentachloride with a concentrated ammonium solution.*

Keywords: *molybdenum, oxides, thermal analysis, X-ray diffraction analysis, IR spectroscopy, particle size analysis.*

For citation: Nikishina E.E., Lebedeva E.N., Drobot D.V. Molybdenum(VI) oxide: New methods of synthesis and properties. *Tonk. Khim. Tekhnol. = Fine Chem. Technol.* 2020;15(2):67-76. https://doi.org/10.32362/2410-6593-2020-15-2-67-76

Оксид молибдена(VI): Новые методы синтеза и свойства

Е.Е. Никишина[@], Е.Н. Лебедева, Д.В. Дробот

МИРЭА – Российский технологический университет (Институт тонких химических технологий имени М.В. Ломоносова), Москва, 119454 Россия
[@]Автор для переписки, e-mail: helena_nick@mail.ru

Цели. *Целью работы была разработка новых методов синтеза оксида молибдена(VI), являющегося предшественником для синтеза функциональных материалов на его основе, а также исследование физико-химических свойств полученных фаз.*

Методы. *Синтезированные фазы и продукты их термолиза изучали методами дифференциально-термического анализа, ИК-спектроскопии, рентгенофазового анализа, гранулометрии.*

Результаты. *Разработаны три метода синтеза оксида молибдена(VI) и исследованы физико-химических свойства полученных оксидных фаз. Первый способ заключался во взаимодействии пентахлорида молибдена с раствором аммиака концентрацией 6.0–9.5 моль/л, второй – во взаимодействии пентахлорида ниобия с раствором серной кислоты, третий – во взаимодействии молибдата аммония с азотной кислотой. В первом случае образовался гидроксид молибдена(V) $MoO(OH)_3$ бурого цвета, во втором случае наблюдалось образование осадка ярко-синего цвета – молибденовой сини $MoO_{2.75}$, в третьем случае образовался гидратированный оксид $MoO_3{\cdot}H_2O$ белого цвета.*

Выводы. *Дифференциально-термический и рентгенофазовый анализы показали, что во всех случаях образцы представляют собой аморфные фазы. Термическая обработка (T = 580 °C) синтезированных фаз приводит к образованию триоксида молибдена ромбической модификации. Для всех продуктов термолиза рассчитаны параметры решетки и рентгеновская плотность. Проведено исследование влияния термической обработки на размер частиц синтезированных образцов и продуктов их термолиза. Гранулометрический анализ показал, что в зависимости от способа получения триоксида молибдена, образуются частицы разного диаметра. Наименьший размер частиц (0.3–0.6 мкм) обнаружен у триоксида молибдена – продукта термолиза образца, полученного при взаимодействии пентахлорида молибдена с концентрированным раствором аммиака.*

Ключевые слова: *молибден, оксиды, термический анализ, рентгенофазовый анализ, ИК-спектроскопия, гранулометрический анализ.*

Для цитирования: Никишина Е.Е., Лебедева Е.Н., Дробот Д.В. Оксид молибдена(VI): Новые методы синтеза и свойства. *Тонкие химические технологии.* 2020;15(2):67-76. https://doi.org/10.32362/2410-6593-2020-15-2-67-76

INTRODUCTION

Molybdenum forms compounds having a wide variety of metal oxidation states, which results in oxide phases that are characterized by a rich chemistry. Despite the increased interest in the oxide phases of molybdenum, especially in MoO_2 and MoO_3, the available information about their properties is still scarce. Further study of the oxides of molybdenum is essential for the development of new applications in modern industry. In particular, these compounds are potential candidates for efficient electrochemical energy storage systems due to their unique physical and chemical properties such as conductivity and mechanical and thermal stability [1–4].

Figure 1 shows the phase diagram of the molybdenum–oxygen system.

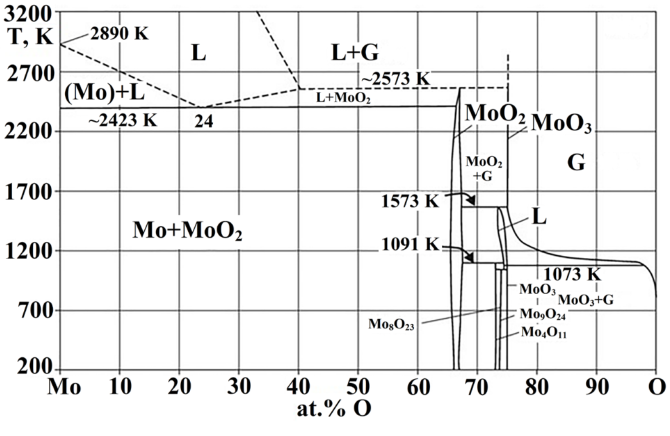

Fig. 1. Phase diagram of the molybdenum–oxygen system [5].

The stable oxides of this system are the α-phase of molybdenum trioxide (MoO_3) and the δ-phase of molybdenum dioxide (MoO_2). Additionally, there are eight phases of intermediate composition between MoO_3 and MoO_2: Mo_4O_{11}, Mo_5O_{14}, Mo_6O_{17}, Mo_7O_{20}, Mo_8O_{23}, Mo_9O_{26}, $Mo_{17}O_{47}$, and $Mo_{18}O_{52}$. These phases have a pronounced nonstoichiometry, and most of them are unstable. For example, the Mo_4O_{11} phase disproportionates into MoO_2 and MoO_3. The bonds in oxides are mainly ionic, but also partially covalent; the volatility of oxides confirms the covalent nature of their bonds [5–8].

Molybdenum(IV) oxide crystallizes in a distorted rutile-type monoclinic lattice (a = 0.5611 nm, b = 0.4856 nm, c = 0.5628 nm). This oxide has a chain structure consisting of MoO_6 octahedra that are connected by common edges and vertices (Fig. 2) [5, 9].

Molybdenum(VI) oxide consists of white, green-tinged, flat rhombic crystals (a = 0.3963 nm, b = 1.3855 nm, c = 0.3696 nm) with a layered structure. In the MoO_3 molecule, the coordination number of molybdenum is six. Its structure, which is similar to that of crystalline ReO_3, is constructed from coordination polyhedra that can be joined by vertices, edges, or both. The unequal number of molybdenum–oxygen bonds connected by vertices and edges leads to a strongly distorted octahedral coordination around the metal centers. Each molybdenum atom is located in the center of a MoO_6 octahedron and surrounded by six oxygen atoms, which are located at the vertices of the octahedron. MoO_3 has several polymorphic modifications (Fig. 3): the most thermodynamically stable phase α-MoO_3 (*Pnma* space group), the metastable modification β-MoO_3, and h-MoO_3. In the α-MoO_3 and h-MoO_3 modifications, the MoO_6 octahedra are linked to each other by both vertices and edges, whereas they are linked only by the vertices in β-MoO_3 [5, 10–12].

The unique layered structure of MoO_3 renders it a promising material for anode and cathode in electrochemical capacitors [4]. Catalytic materials based on MoO_3 have been used in processes such as methanol oxidation, isomerization and hydrogenation of olefins, and oil refining (cracking, hydrotreating, and reforming) [13, 14]. Currently, the production of MoO_3-based materials is carried out via a limited number of methods including chemical deposition, hydrothermal process, sol–gel method, or chemical vapor deposition [15–20], most of which require high temperatures and pressures.

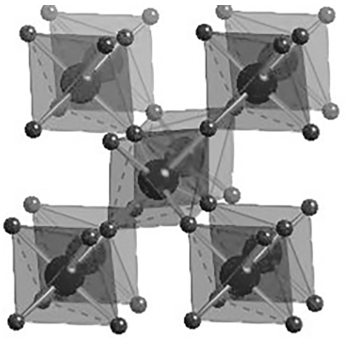

Fig. 2. Structure of molybdenum dioxide. Oxygen atoms are located at the vertices of octahedra, and molybdenum atoms are located in the center of octahedra [5].

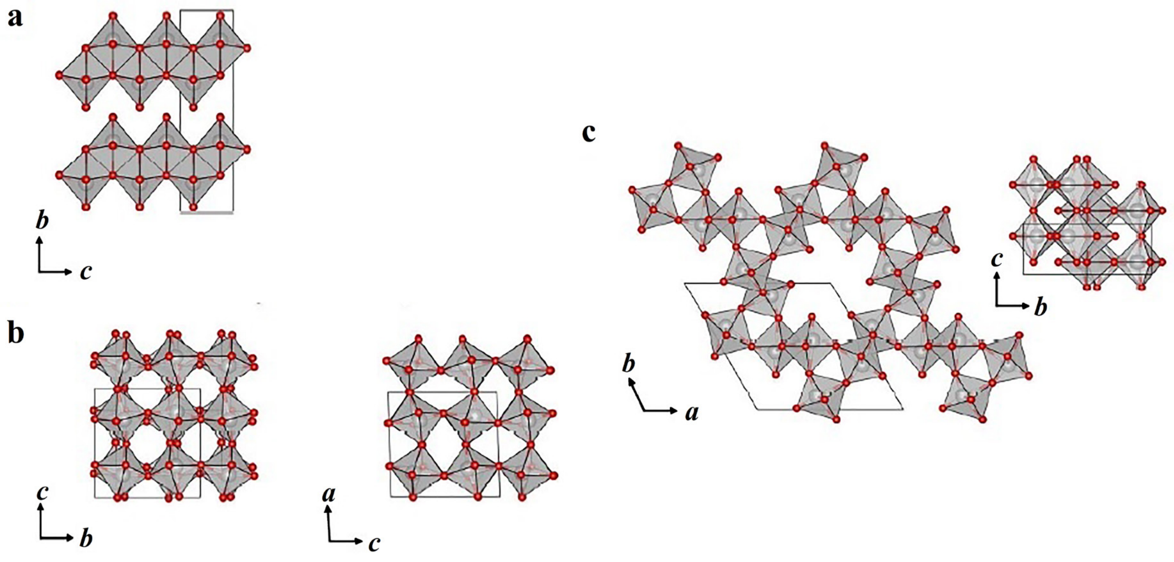

Fig. 3. Structures of polymorph modifications of molybdenum trioxide: a) α-MoO_3, b) β-MoO_3, c) h-MoO_3. In all structures, a unit cell is shown as a thin black line, oxygen atoms are indicated by black spheres, molybdenum atoms are located inside the gray MoO_6 octahedra [12].

The aim of this work is to explore new methods for the synthesis of molybdenum(VI) oxide, which is a precursor for the synthesis of functional materials, as well as to study the physical and chemical properties of the resulting phases.

MATERIALS AND METHODS

The precursors used in this work were molybdenum pentachloride (qualification ACS, *Merck*, Germany), ammonium molybdate (qualification AR, *Merck*, Germany), sulfuric acid (qualification CP, GOST 4204-77, *CHIMMED*, Russia), nitric acid (qualification ACS, GOST 11125-84, *CHIMMED*, Russia), and ammonia solution (qualification ACS 25-5, GOST 24147-80, *CHIMMED*, Russia).

Molybdenum oxide phases were obtained by the three following synthesis methods:

- The first synthesis consisted in the reaction of molybdenum pentachloride with a 6.0–9.5 mol/L ammonia solution. In this case, a brown precipitate was formed, which was indicative of the formation of molybdenum(V) hydroxide $MoO(OH)_3$ according to reaction (1) as follows [21]:

$$MoCl_5 + 5NH_3{\cdot}H_2O \rightarrow MoO(OH)_3 + 5NH_4Cl + H_2O \quad (1)$$

- In the second synthetic procedure, a solution of concentrated sulfuric acid was added to molybdenum pentachloride. During this reaction, the formation of a bright blue precipitate was observed, which corresponds most likely to molybdenum blue. This compound, in which molybdenum exhibits the oxidation states +5 and +6, is usually obtained by reducing molybdenum(VI) to molybdenum(V) [22, 23]. In contrast, we oxidized molybdenum(V) to molybdenum(VI) using sulfuric acid as a strong oxidizer according to reaction (2):

$$4MoCl_5 + 2H_2SO_4 + 9H_2O \rightarrow 4MoO_{2.75} + SO_2 + 20HCl \quad (2)$$

- The third synthesis consisted in the reaction of ammonium molybdate with boiling nitric acid as follows:

$$(NH_4)_2MoO_4 + 2HNO_3 \rightarrow MoO_3{\cdot}nH_2O + 2NH_4NO_3 \quad (3)$$

As a result, a fine white powder was formed.

Differential thermal analysis of the samples was performed on a Q-1500 D derivatograph (F. Paulik, J. Paulik, L. Erdey; *MOM*, Hungary) in air with the simultaneous recording of four curves, namely, differential (DTA), thermal (T), differential thermogravimetric (DTG), and integral weight loss (TG) curves using the software and hardware systems developed by *IP Tetran*, Russia, in the LabVIEW 8.21 environment (*National Instruments*, Austin, Texas, USA). The temperature was measured using a PP-1 platinum/platinum–rhodium thermocouple with an error of ±5°C within a temperature range of 20–1000°C, at a heating rate of 10°C/min, and using α-Al_2O_3 as a reference sample.

X-ray diffraction (XRD) analysis was performed on a Bruker D8 Advance diffractometer using CuK_α radiation, continuous sample rotation (1°/min), and step-by-step (step 2θ = 0.02°, exposure 0.5 s/step) mode in the angle range 2θ = 5–80°. The International Center for Diffraction Data–Joint Committee on Power Diffraction Standards (ICDD–JCPDS) card file was used for phase identification.

The X-ray density was calculated using the formula:

$$\rho_{X-ray} = \frac{M \times Z \times 1.66}{V}\,, \quad (4)$$

where M is the molecular weight, g/mol; Z is the number of formula units; and V is the volume of the unit cell, Å^3.

In the case of the rhombic modification of molybdenum trioxide ($a \neq b \neq c$, $\alpha = \beta = \gamma = 90°$), the following formula applies:

$$V = a \times b \times c\,. \quad (5)$$

Infrared (IR) absorption spectra in the area of 3600–400 cm^{-1} were recorded on a Specord M80 spectrometer by using KBr pellets, with an error below 3–4 cm^{-1}.

Granulometric analysis for the determination of the particle size distribution was performed using a DelsaNano laser particle analyzer from *Beckman Coulter*, USA. This device can measure particles dispersed in a liquid in the measurement range from 0.6 nm to 7 µm by diffraction method. The LS series devices use laser light with a wavelength of 780 nm.

Heat treatment of samples was carried out in a laboratory furnace TK-12.1250.H.1Ф equipped with an automatic temperature controller "Thermomatic-N." The error of automatic control at the nominal temperature was ±1°C.

RESULTS AND DISCUSSION

The thermal transformations of the synthesized phases were studied in the temperature range from 20 to 1000°C.

Figure 4 shows the DTA curves of the samples.

The DTA curves demonstrate the occurrence of endothermic effects associated with a dehydration

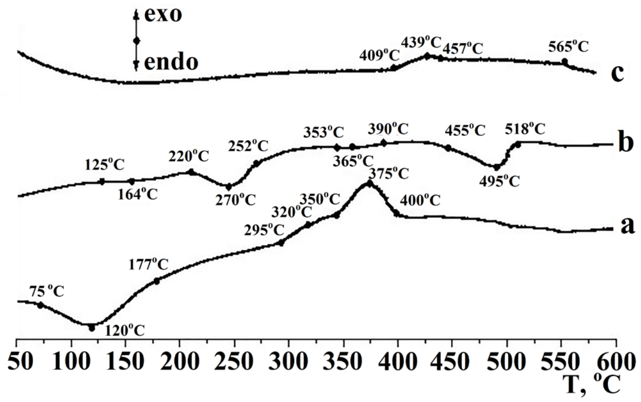

Fig. 4. Differential thermal analysis curves of
a) the sample obtained by the reaction of molybdenum(V) chloride with a concentrated ammonium solution (brown powder),
b) the sample obtained by the reaction of molybdenum(V) chloride with a concentrated sulfuric acid solution (molybdenum blue),
and c) the sample obtained by the reaction between ammonium molybdate and nitric acid.

process. In addition, for the sample obtained by reacting molybdenum(V) chloride with a concentrated sulfuric acid solution, the observed endothermic effects may be associated with the volatilization of reaction byproducts such as SO_2 and HCl. The presence of an exothermic effect at 350–400°C (Fig. 4a) corresponds to the oxidation process of Mo(V) to Mo(VI), which was confirmed by the increase in the mass of the sample during the annealing process. An exothermic effect in the temperature range of 410–460°C for the sample obtained by the reaction between ammonium molybdate and nitric acid (Fig. 4c) can be attributed to the decomposition of the reaction byproduct, i.e., molybdenum oxonitrate $MoO_2(NO_3)_2$, to nitrogen dioxide (NO_2) and molybdenum oxide (MoO_3). This process was accompanied by a decrease in the mass of the sample. Moreover, an exothermic effect in the temperature range of 555–565°C can be assigned to the crystallization of amorphous molybdenum trioxide.

At temperatures above 600°C, a significant decrease in mass was observed for all samples due to evaporation of molybdenum(VI) oxide. According to the literature, this compound begins to evaporate below its melting point (in the range of 600–795°C). Thus, a noticeable increase in pressure occurs at the melting temperature (795°C) [24].

On the basis of the IR spectroscopy and XRD results, we decided to anneal the samples at 580°C because the mass of the samples remains constant at this temperature, and the evaporation process has not yet begun.

Similar absorption bands are observed in the IR spectra of the three samples. In particular, the residual absorption band in the region of 3600–3000 cm^{-1}, with a maximum at ~3465 cm^{-1}, is attributable to valence vibrations of hydroxo groups and water (Fig. 5) [25]. The absorption band at 993–987 cm^{-1} corresponds to the Mo=O bonds. This band is characteristic of crystalline MoO_3, in which each molybdenum atom is surrounded by six oxygen atoms, thus forming a MoO_6 octahedron [26]. The absorption bands in the 880–860 cm^{-1} region correspond to symmetrical Mo–O–Mo vibrations, and the absorption band at 820 cm^{-1} corresponds to asymmetric Mo–O–Mo vibrations of molybdenum trioxide, in which the oxygen atom bridges two MoO_6 octahedra [27]. The absorption band at 623–583 cm^{-1} corresponds to Mo_3–O vibrations. In this case, the oxygen atom is shared between three MoO_6 octahedra [27, 28].

Then, the samples were subjected to isothermal annealing at 580°C for 15 hours. The annealing temperature was selected according to the results of differential thermal analysis; at 580°C, the loss of mass was completed. The resulting phases were gray-green powders.

To identify the obtained phases, the synthesized samples and their thermolysis products were subjected to an XRD analysis at 580°C. All the synthesized samples were amorphous phases.

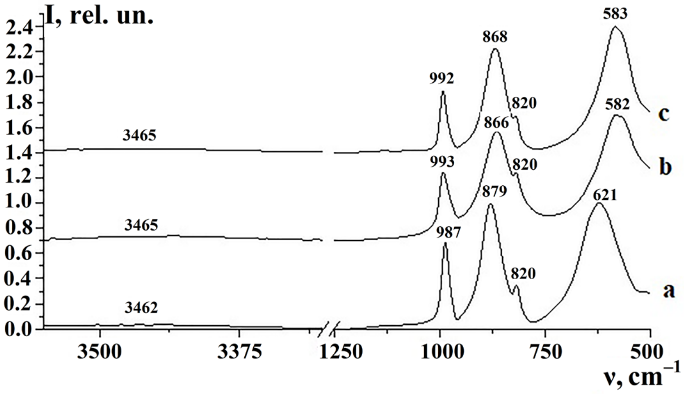

Fig. 5. IR spectra of the products of the thermal decomposition of
a) the sample obtained by the reaction of molybdenum(V) chloride with a concentrated ammonia solution (brown powder),
b) the sample obtained by the reaction of molybdenum(V) chloride with a concentrated sulfuric acid solution (molybdenum blue),
and c) the sample obtained by the reaction between ammonium molybdate and nitric acid.

The XRD patterns of the thermal decomposition products (T = 580°C) are shown in Fig. 6. In all cases, the formation of a rhombic modification of molybdenum oxide MoO_3 can be observed. The unit cell parameters and X-ray density are summarized in table.

The influence of heat treatment on the particle size of the synthesized samples and their thermolysis products at 580°C was studied. Figure 7a shows the particle size distribution of the sample obtained by reacting molybdenum pentachloride with an ammonia solution. The main fraction corresponds to a particle size of 0.7–1.2 µm (~90%). Upon heat treatment of this sample, molybdenum trioxide having particles of 0.3–0.6 µm (~95%) was obtained (Fig. 7b). Unfortunately, the determination of the particle size of the sample obtained by reaction of molybdenum pentachloride with a sulfuric acid solution was hindered by its solubility in water.

Figure 8 shows the particle size distribution of the thermolysis product of this sample. The main fraction corresponds to a particle size of 0.6–0.9 µm (~95%).

Figure 9a shows the particle size distribution of a sample obtained by reacting ammonium molybdate with a nitric acid solution. The main fraction corresponds to particles with a size of 3.0–5.0 µm (~90%). During heat treatment of the sample, molybdenum trioxide having two particle fractions, i.e., particles of 0.7–1.0 µm (~80%) and 3.0–6.0 µm (~6%), was obtained (Fig. 9b).

As can be seen from the particle distributions, the smallest particles were formed upon thermolysis of the sample obtained by reacting molybdenum pentachloride with an ammonia solution.

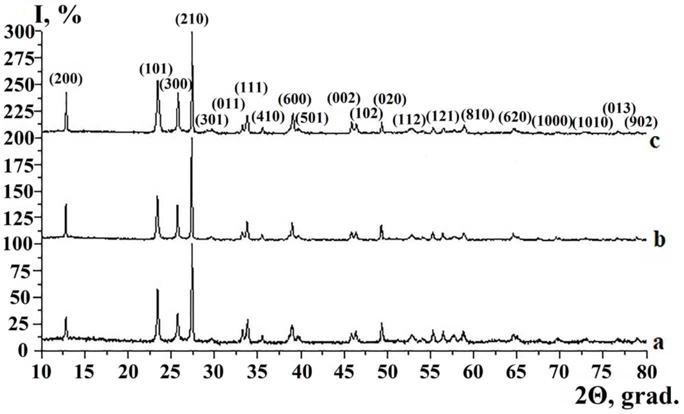

Fig. 6. X-ray diffraction patterns of the products obtained after thermal decomposition at 580°C for 15 hours of
a) the sample obtained by the reaction of molybdenum(V) chloride with a concentrated ammonia solution (brown powder),
b) the sample obtained by the reaction of molybdenum(V) chloride with a concentrated sulfuric acid solution (molybdenum blue),
and c) the sample obtained by the reaction between ammonium molybdate and nitric acid.

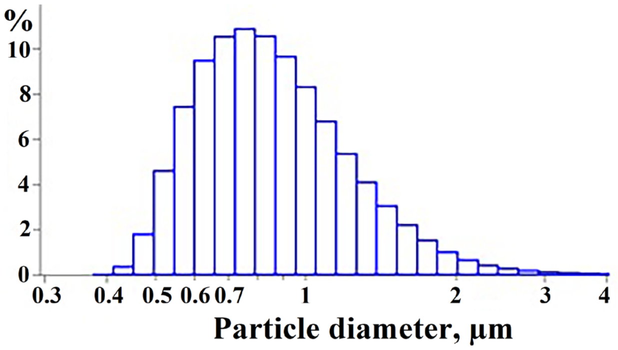

Fig. 8. Particle size distribution of the product of the thermolysis of the sample obtained by the reaction of molybdenum pentachloride with a sulfuric acid solution.

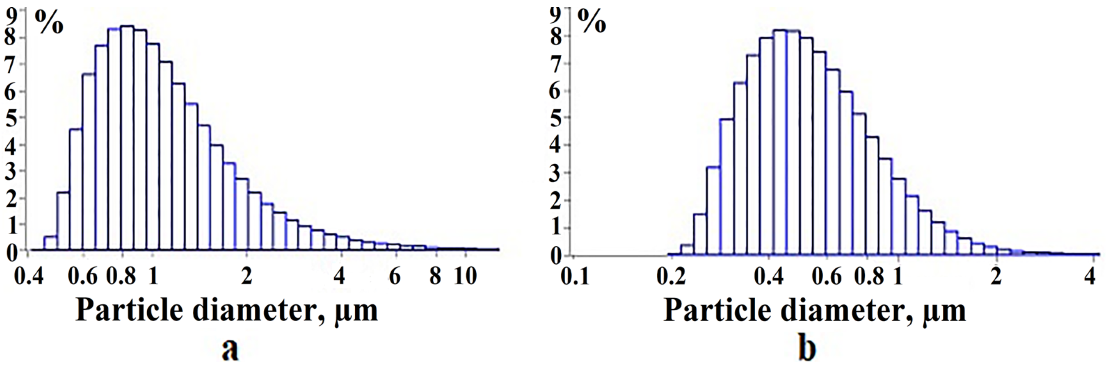

Fig. 7. Particle size distribution of (a) the sample obtained by the reaction of molybdenum pentachloride with an ammonia solution and (b) the product of its heat treatment at T = 580°C.

XRD data of the samples obtained after annealing at 580°C

Lattice parameters of the synthesized samples		**ICDD–JCPDS data for MoO_3 (orthorhombic)**
Synthesis 1 (molybdenum pentachloride and ammonia solution)	$a = (1.382 \pm 0.001)$ nm $b = (0.3696 \pm 0.0005)$ nm $c = (0.3956 \pm 0.0005)$ nm $V = 202.07 \times 10^{-3}$ nm^3 $\rho_{X\text{-}ray} = 4.73$ g/cm^3	$a = 1.3825$ nm $b = 0.3694$ nm $c = 0.3954$ nm $V = 201.93 \times 10^{-3}$ nm^3 $\rho_{X\text{-}ray} = 4.73$ g/cm^3
Synthesis 2 (molybdenum pentachloride and sulfuric acid)	$a = (1.383 \pm 0.001)$ nm $b = (0.3699 \pm 0.0005)$ nm $c = (0.3960 \pm 0.0005)$ nm $V = 202.70 \times 10^{-3}$ nm^3 $\rho_{X\text{-}ray} = 4.54$ g/cm^3	
Synthesis 3 (ammonium molybdate and nitric acid)	$a = (13.817 \pm 0.01)$ nm $b = (3.694 \pm 0.001)$ nm $c = (3.959 \pm 0.005)$ nm $V = 202.07 \times 10^{-3}$ nm^3 $\rho_{X\text{-}ray} = 4.73$ g/cm^3	

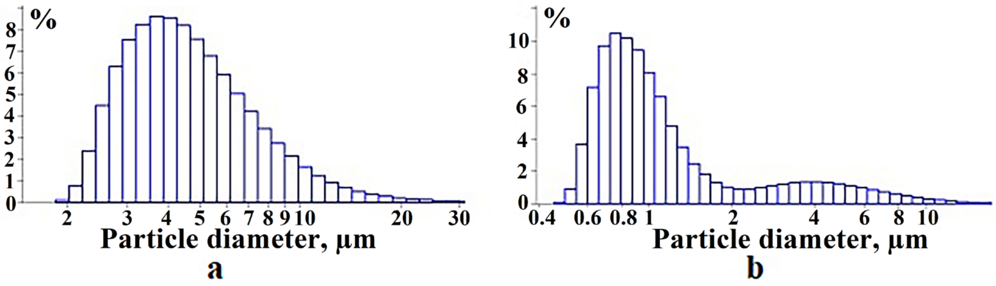

Fig. 9. Particle size distribution of (a) the sample obtained by the reaction of ammonium molybdate with nitric acid and (b) the product of its heat treatment at T = 580°C.

CONCLUSIONS

1. Oxide phases in the molybdenum–oxygen system were synthesized following three procedures. The first method consists in the heterophase reaction of molybdenum pentachloride with a concentrated ammonia solution, the second in the reaction of molybdenum pentachloride with a concentrated sulfuric acid solution, and the third in the reaction of nitric acid with ammonium molybdate.
2. Using various analytical methods including XRD, DTA-DTG, IR spectroscopy, and granulometry, the physicochemical properties of the synthesized samples and their thermolysis products were studied.
3. DTA and XRD analysis demonstrated that in all cases the samples were amorphous phases. Heat treatment at 580°C led to the formation of a rhombic modification of molybdenum trioxide. Lattice parameters and X-ray density were calculated for all thermolysis products.
4. The results of granulometric analysis showed that particles of different diameters were formed depending on the synthetic method. The smallest particle size (0.3–0.6 µm) was found in molybdenum trioxide, a thermolysis product of the sample obtained by reacting molybdenum pentachloride with a concentrated ammonia solution.

Acknowledgments

This work was supported by the Russian Foundation for Basic Research, project No. 18-03-00671.

The authors declare no conflicts of interest.

REFERENCES

1. Miao F., Wu W., Li Q., Miao R., Tao B. Fabrication and Application of Molybdenum Trioxide Nanostructure Materials for Electrochemical Capacitors. *Int. J. Electrochem. Sci.* 2017;12:12060-12073.
https://doi.org/10.20964/2017.12.200

2. Ban D., Xu N., Deng S., Chen J., She J. Low-temperature Synthesis of Large-area Films of Molybdenum Trioxide Microbelts in Air and the Dependence of Their Field Emission Performance on Growth Conditions. *J. Mater. Sci. Technol.* 2010;26(7):584-588.
https://doi.org/10.1016/S1005-0302(10)60089-8

3. Li G., Jiang L., Pang S., Peng H. Zhang Z. Molybdenum Trioxide Nanostructures: The Evolution from Helical Nanosheets to Crosslike Nanoflowers to Nanobelts. *J. Phys. Chem. B.* 2006;110(48):24472-24475.
https://doi.org/10.1021/jp064855v

4. Hu X., Zhang W., Liu X., Meia Y., Huang Y. Nanostructured Mo-based electrode materials for electrochemical energy storage. *Chem. Soc. Rev.* 2015;44(8):2376-2404.
https://doi.org/10.1039/C4CS00350K

5. Predel F. Phase diagram of Mo–O (molybdenum–oxygen) system. In: Predel F. (eds.) Phase Equilibria, Crystallographic and Thermodynamic Data of Binary Alloys. Physical Chemistry. Berlin, Heidelberg: Springer; 2016. V. 12D.

6. Karelin V.A. *Himiya i tekhnologiya molibdena i vol'frama* (Chemistry and technology molybdenum and tungstem). Tomsk: Tomsk Polytechnic University; 2017. 58 p. (in Russ.).

7. Henrich V.E., Cox P.A. The surface science of metal oxides. Cambridge: Cambridge University Press; 1996. 480 p.

8. Kihlborg L. Studies on molybdenum oxides. *Acta Chem. Scand.* 1959;13:954-962.
https://doi.org/10.3891/acta.chem.scand.13-0954

9. Brandt B.G. Skapski A.C. A refinement of the crystal structure of molybdenum dioxide. *Acta Chem. Scand.* 1967;21:661-672.
https://doi.org/10.3891/acta.chem.scand.21-0661

10. Tsuda N., Nasu K., Fujimori A., Siratori K. Electronic conduction in oxides. New York: Springer-Verlag; 1991. 323 p.

11. Kihlbord L. Least squares refinement of the crystal structure of molybdenum. *Arkiv för Kemi.* 1963;21:357-364.

12. Yun J., Jang W., Lee T., Lee Y., Soon A. Aligning the band structures of polymorphic molybdenum oxides and organic emitters in light-emitting diodes. *Phys. Rev. Applied.* 2017;7:024025-1-024025-8.
https://doi.org/10.1103/PhysRevApplied.7.024025

13. Mendes F.M. Weibel D.E., Blum R.P., Middeke J. Preparation and characterization of well-ordered MoO_x films on $Cu_3Au(100)$–oxygen substrate (CAOS). *Catal. Today.* 2008;133(1):187-191.
https://doi.org/10.1016/j.cattod.2007.11.046

14. Tomina N.N., Pimerzin A.A., Moiseev I.K. Sulfide catalysts for hydropurification of oil fractions. *Russ. J. Gen. Chem.* 2009;79(6):1274-1288.
https://doi.org/10.1134/S1070363209060449

15. Méndez-Vivar J. Synthesis of molybdenum oxides by the sol-gel method. *Inorg. Chim. Acta.* 1991;179(1):77-82.
https://doi.org/10.1016/S0020-1693(00)85376-1

16. Ganguly A., George R. Synthesis, characterization and gas sensitivity of MoO_3 nanoparticles. *Bull. Mater. Sci.* 2007;30(2):183-185.
https://doi.org/10.1007/s12034-007-0033-6

СПИСОК ЛИТЕРАТУРЫ

1. Miao F., Wu W., Li Q., Miao R., Tao B. Fabrication and Application of Molybdenum Trioxide Nanostructure Materials for Electrochemical Capacitors. *Int. J. Electrochem. Sci.* 2017;12:12060-12073.
https://doi.org/10.20964/2017.12.200

2. Ban D., Xu N., Deng S., Chen J., She J. Low-temperature Synthesis of Large-area Films of Molybdenum Trioxide Microbelts in Air and the Dependence of Their Field Emission Performance on Growth Conditions. *J. Mater. Sci. Technol.* 2010;26(7):584-588.
https://doi.org/10.1016/S1005-0302(10)60089-8

3. Li G., Jiang L., Pang S., Peng H. Zhang Z. Molybdenum Trioxide Nanostructures: The Evolution from Helical Nanosheets to Crosslike Nanoflowers to Nanobelts. *J. Phys. Chem. B.* 2006;110(48):24472-24475.
https://doi.org/10.1021/jp064855v

4. Hu X., Zhang W., Liu X., Meia Y., Huang Y. Nanostructured Mo-based electrode materials for electrochemical energy storage. *Chem. Soc. Rev.* 2015;44(8):2376-2404.
https://doi.org/10.1039/C4CS00350K

5. Predel F. Phase diagram of Mo–O (molybdenum–oxygen) system. In: Predel F. (eds.) Phase Equilibria, Crystallographic and Thermodynamic Data of Binary Alloys. Physical Chemistry. Berlin, Heidelberg: Springer; 2016. V. 12D.

6. Карелин В.А. Химия и технология молибдена и вольфрама. Томск: изд-во Томского политехнического университета; 2017. 58 с.

7. Henrich V.E., Cox P.A. The surface science of metal oxides. Cambridge: Cambridge University Press; 1996. 480 p.

8. Kihlborg L. Studies on molybdenum oxides. *Acta Chem. Scand.* 1959;13:954-962.
https://doi.org/10.3891/acta.chem.scand.13-0954

9. Brandt B.G., Skapski A.C. A refinement of the crystal structure of molybdenum dioxide. *Acta Chem. Scand.* 1967;21:661-672.
https://doi.org/10.3891/acta.chem.scand.21-0661

10. Tsuda N., Nasu K., Fujimori A., Siratori K. Electronic conduction in oxides. New York: Springer-Verlag; 1991. 323 p.

11. Kihlbord L. Least squares refinement of the crystal structure of molybdenum. *Arkiv för Kemi.* 1963;21:357-364.

12. Yun J., Jang W., Lee T., Lee Y., Soon A. Aligning the band structures of polymorphic molybdenum oxides and organic emitters in light-emitting diodes. *Phys. Rev. Applied.* 2017;7:024025-1-024025-8.
https://doi.org/10.1103/PhysRevApplied.7.024025

13. Mendes F.M. Weibel D.E., Blum R.P., Middeke J. Preparation and characterization of well-ordered MoOx films on $Cu_3Au(100)$–oxygen substrate (CAOS). *Catal. Today.* 2008;133(1):187-191.
https://doi.org/10.1016/j.cattod.2007.11.046

14. Tomina N.N., Pimerzin A.A., Moiseev I.K. Sulfide catalysts for hydropurification of oil fractions. *Russ. J. Gen. Chem.* 2009;79(6):1274-1288.
https://doi.org/10.1134/S1070363209060449

15. Méndez-Vivar J. Synthesis of molybdenum oxides by the sol-gel method. *Inorg. Chim. Acta.* 1991;179(1):77-82.
https://doi.org/10.1016/S0020-1693(00)85376-1

16. Ganguly A., George R. Synthesis, characterization and gas sensitivity of MoO_3 nanoparticles. *Bull. Mater. Sci.* 2007;30(2):183-185.
https://doi.org/10.1007/s12034-007-0033-6

17. Pergament A.L., Malinenko V.P., Aleshina L.A., Kazakova E.L., Kuldin N.A. Electrical switching in thin film structures based on molybdenum oxides. *J. Exp. Phys.* 2014;2014:6 p. https://doi.org/10.1155/2014/951297

18. Chiang T.H., Yeh H.C. The synthesis of α-MoO_3 by ethylene glycol. *Materials.* 2013;6(10):4609-4625. https://doi.org/10.3390/ma6104609

19. Parviz D., Kazemeini M., Rashidi A.M., Jozani J. Synthesis and characterization of MoO_3 nanostructures by solution combustion method employing morphology and size control. *J. Nanopart. Res.* 2010;12(4):1509-1521. https://doi.org/10.1007/s11051-009-9727-6

20. Siciliano T., Tepore A., Filippo E., Micocci G., Tepore M. Characteristics of molybdenum trioxide nanobelts prepared by thermal evaporation technique. *Mater. Chem. Phys.* 2009;114(2-3):687-691. https://doi.org/10.1016/j.matchemphys.2008.10.018

21. Gupta C.K. Extractive metallurgy of molybdenum. Boca Raton: CRC Press; 1992. 404 p.

22. Nakamura I., Miras H.N., Fujiwara A., Fujibayashi M., etc. Investigating the formation of “molybdenum blues” with gel electrophoresis and mass spectrometry. *J. Am. Chem. Soc.* 2015;137(20):6524-6530. https://doi.org/10.1021/ja512758j

23. Koyun O., Gorduk S., Arvas M.B., Sahin Y. Direct, one-step synthesis of molybdenum blue using an electrochemical method, and characterization studies. *Synth. Met.* 2017;233:111-118. https://doi.org/10.1016/j.synthmet.2017.09.009

24. Kazenas E.K., Tsvetkov Yu.V. *Isparenie oksidov* (Evaporation of oxides). Moscow: Nauka; 1997. 543 p. (in Russ.).

25. Yuhnevich Yu.G. Advances in the use of IR-spectroscopy to characterize OH bonds. *Uspekhi Khimii = Russ. Chem. Rev.* 1963;32(11):1397-1423 (in Russ.).

26. Li C., Xin Q., Wang K.-L., Guo X. FT-IR Emission spectroscopy studies of molybdenum oxide and supported molybdena on alumina, silica, zirconia, and titania. *Appl. Spectrosc.* 1991;45(5):874-882. https://doi.org/10.1366/0003702914336651

27. Chen D., Liu M., Yin L., Li T. *et al.* Single-crystalline MoO_3 nanoplates: topochemical synthesis and enhanced ethanol-sensing performance. *J. Mater. Chem.* 2011;21(25):9332-9342. https://doi.org/10.1039/C1JM11447F

28. Pavlova S.S., Kotvanova M.K. IR-spectra and electromechanical properties of transition metal oxide bronzes. *Vestnik Yugorskogo gosudarstvennogo universiteta = Yugra State University Bulletin.* 2008;10(3):61-63 (in Russ.).

17. Pergament A.L., Malinenko V.P., Aleshina L.A., Kazakova E.L., Kuldin N.A. Electrical switching in thin film structures based on molybdenum oxides. *J. Exp. Phys.* 2014;2014:6 p. https://doi.org/10.1155/2014/951297

18. Chiang T.H., Yeh H.C. The synthesis of α-MoO_3 by ethylene glycol. *Materials.* 2013;6(10):4609-4625. https://doi.org/10.3390/ma6104609

19. Parviz D., Kazemeini M., Rashidi A.M., Jozani J. Synthesis and characterization of MoO_3 nanostructures by solution combustion method employing morphology and size control. *J. Nanopart. Res.* 2010;12(4):1509-1521. https://doi.org/10.1007/s11051-009-9727-6

20. Siciliano T., Tepore A., Filippo E., Micocci G., Tepore M. Characteristics of molybdenum trioxide nanobelts prepared by thermal evaporation technique. *Mater. Chem. Phys.* 2009;114(2-3):687-691. https://doi.org/10.1016/j.matchemphys.2008.10.018

21. Gupta C.K. Extractive metallurgy of molybdenum. Boca Raton: CRC Press; 1992. 404 p.

22. Nakamura I., Miras H.N., Fujiwara A., Fujibayashi M., etc. Investigating the formation of «molybdenum blues» with gel electrophoresis and mass spectrometry. *J. Am. Chem. Soc.* 2015;137(20):6524-6530. https://doi.org/10.1021/ja512758j

23. Koyun O., Gorduk S., Arvas M.B., Sahin Y. Direct, one-step synthesis of molybdenum blue using an electrochemical method, and characterization studies. *Synth. Met.* 2017;233:111-118. https://doi.org/10.1016/j.synthmet.2017.09.009

24. Казенас Е.К., Цветков Ю.В. Испарение оксидов. М.: Наука; 1997. 543 с.

25. Юхневич Ю.Г. Успехи в применении ИК-спектроскопии для характеристики ОН-связей. *Успехи химии.* 1963;32(11):1397-1423.

26. Li C., Xin Q., Wang K.-L., Guo X. FT-IR Emission spectroscopy studies of molybdenum oxide and supported molybdena on alumina, silica, zirconia, and titania. *Appl. Spectrosc.* 1991;45(5):874-882. https://doi.org/10.1366/0003702914336651

27. Chen D., Liu M., Yin L., Li T. *et al.* Single-crystalline MoO_3 nanoplates: topochemical synthesis and enhanced ethanol-sensing performance. *J. Mater. Chem.* 2011;21(25):9332-9342. https://doi.org/10.1039/C1JM11447F

28. Павлова С.С., Котванова М.К. ИК-спектры и электромеханические свойства оксидных бронз переходных металлов. *Вестник Югорского государственного университета.* 2008;10(3):61-63.

About the authors:

Elena E. Nikishina, Assistant Professor, Department of Chemistry and Technology Rare and Dispersed Elements, Nanoscale and Composite Materials, M.V. Lomonosov Institute of Fine Chemical Technologies, MIREA – Russian Technological University (86, Vernadskogo pr., Moscow, 119571, Russia). E-mail: nikishina@mirea.ru. Scopus Author ID 6602839662, ResearherID O-7115-2014, https://orcid.org/0000-0003-3579-2194

Elena N. Lebedeva, Engineer, Department of Chemistry and Technology Rare and Dispersed Elements, Nanoscale and Composite Materials, M.V. Lomonosov Institute of Fine Chemical Technologies, MIREA – Russian Technological University (86, Vernadskogo pr., Moscow, 119571, Russia). E-mail: rare214@mail.ru. Scopus Author ID 7102162057, https://orcid.org/0000-0003-1532-8845

Dmitry V. Drobot, Professor, Department of Chemistry and Technology Rare and Dispersed Elements, Nanoscale and Composite materials, M.V. Lomonosov Institute of Fine Chemical Technologies, MIREA – Russian Technological University (86, Vernadskogo pr., Moscow, 119571, Russia). E-mail: dvdrobot@mail.ru. Scopus Author ID 35580931100, https://orcid.org/0000-0002-0379-2926

Об авторах:

Никишина Елена Евгеньевна, доцент кафедры химии и технологии редких и рассеянных элементов, наноразмерных и композиционных материалов Института тонких химических технологий им. М.В. Ломоносова ФГБОУ ВО «МИРЭА – Российский технологический университет» (119571, Россия, Москва, пр-т Вернадского, д. 86). E-mail: nikishina@mirea.ru. Scopus Author ID 6602839662, ResearherID O-7115-2014, https://orcid.org/0000-0003-3579-2194

Лебедева Елена Николаевна, инженер кафедры химии и технологии редких и рассеянных элементов, наноразмерных и композиционных материалов Института тонких химических технологий им. М.В. Ломоносова ФГБОУ ВО «МИРЭА – Российский технологический университет» (119571, Россия, Москва, пр-т Вернадского, д. 86). E-mail: rare214@mail.ru. Scopus Author ID 7102162057, https://orcid.org/0000-0003-1532-8845

Дробот Дмитрий Васильевич, профессор кафедры химии и технологии редких и рассеянных элементов, наноразмерных и композиционных материалов Института тонких химических технологий им. М.В. Ломоносова ФГБОУ ВО «МИРЭА – Российский технологический университет» (119571, Россия, Москва, пр-т Вернадского, д. 86). E-mail: dvdrobot@mail.ru. Scopus Author ID 35580931100, https://orcid.org/0000-0002-0379-2926

Submitted: July 11, 2019; Reviewed: February 10, 2020; Accepted: April 11, 2020.

Translated from Russian into English by N. Isaeva
Edited for English language and spelling by Enago, an editing brand of Crimson Interactive Inc.